Frequency Agile Time Synchronization Procedure for FBMC Waveforms

Jean-Baptiste Doré(✉) and Vincent Berg

CEA-Leti Minatec, 17 rue des Martyrs, 38054 Grenoble Cedex 9, France
jean-baptiste.dore@cea.fr

Abstract. Access to multiple non-contiguous spectrum bands for non-synchronous users is foreseen as essential by some transmission scenarios of the 5^{th} generation of cellular networks (5G). Filterbank Multicarrier modulation (FBMC) has been envisaged because of its ability to give an efficient answer to these requirements. This paper introduces and evaluates the performance of a frequency agile time synchronization solution adapted to FBMC asynchronous transmission on fragmented spectrum. The detection of the start of burst is solely made in the frequency domain assuming that the fast Fourier transform of the receiver is not synchronized. The proposed algorithms have a particular interest for real time implementation when Machine Type Communication applications are considered. This latter scenario is sometimes considered as one of the most challenging for 5G.

Keywords: FBMC · OFDM · Synchronization

1 Introduction

The current generation of cellular physical layers such as used by Long Term Evolution (LTE) and LTE-Advanced have been optimized to deliver high bandwidth pipes to wireless users but require the orthogonality between users within a single cell. More precisely, in case of Orthogonal Frequency Division Multiplexing (OFDM), users should be synchronized in time to avoid inter-user interference. As a consequence LTE networks rely on Timing Advance (TA) value adjustment procedure to manage the synchronization between users.

The expected explosion of Machine-Type-Communication (MTC) is posing new challenges. Fast dormancy necessary for this type of service to save battery power has resulted in significant control signaling growth especially for the TA procedure. Furthermore, as the availability of large amounts of contiguous spectrum is getting more and more difficult to guarantee, the aggregation of non-contiguous frequency bands has to be considered to increase the efficiency of the network.

Therefore relaxed synchronization and access to fragmented spectrum are key parameters for future generations of wireless networks [1]. This requirement of spectrum agility has encouraged the study of alternative multicarrier

D. Noguet et al. (Eds.): CROWNCOM 2016, LNICST 172, pp. 307–318, 2016.
DOI: 10.1007/978-3-319-40352-6_25

waveforms such as Filterbank Multicarrier (FBMC) to provide better adjacent channel leakage performance without compromising spectral efficiency [2]. Frequency Division Multiple Access (FDMA) schemes have already been considered for FBMC modulations [3], and access to fragmented spectrum has been envisaged [4]. When licensed spectrum access is considered, fragmented spectrum is often a consequence of dynamic access to the frequency block. The phenomenon is expected to be further exacerbated when noncontiguous asynchronous dynamic access is considered particularly when messages get shorter as is sometimes the case for MTC applications.

When flexible asynchronous transmission on fragmented spectrum is considered, time synchronization of the multicarrier symbol is not straightforward. Time domain processing is usually considered for multicarrier receivers [5,6]. A signal a priori known to the receiver is initially sent to synchronize the packet. A preamble built on a known sequence (e.g. Zadoff-Chu LTE) or alternatively a training symbol sequence that is repeated n times [6] can be used. When multiple users access the same resource each preamble should be orthogonal to each other. For FDMA, frequency orthogonality usually applies. However, if the synchronization is performed in the time domain, it is difficult to guarantee orthogonality between the users with a reasonable level of complexity, particularly in the considered fragmented spectrum scenario. It requires a per-user filtering process during the synchronization procedure making the time synchronization process ill-adapted to flexible asynchronous fragmented access.

A frequency agile time synchronization solution adapted to the context is investigated in this paper. We propose a frame format associated with a frequency-domain time-synchronization processing particularly adapted to flexible multiuser scenario on fragmented spectrum. Section 2 describes the system model, the frame format and the block diagram of the proposed receiver. In Sect. 3 we derive a time synchronization algorithm and performance is evaluated and discussed. Section 4 concludes the paper.

2 System Model

2.1 FBMC and Proposed Receiver Architecture

A multicarrier system can be described by a synthesis/analysis filter bank, i.e. a transmultiplexer structure. The synthesis filter bank is composed of a set of parallel transmit filters. The analysis filter bank consists of the parallel matched receive filters. The most widely used multicarrier technique is OFDM, based on the use of the inverse and forward Fast Fourier Transform (FFT) for the analysis and the synthesis filter banks. The prototype filter of OFDM is a rectangular window whose size is equal to the duration of the FFT. At the receiver, perfect signal recovery is possible under ideal channel conditions thanks to the orthogonality of the prototype filters. Nevertheless under more realistic multipath channels, a data rate loss has to be paid with the mandatory introduction of a Cyclic Prefix (CP), longer than the impulse response duration of the channel. FBMC waveforms utilize a more advanced prototype filter designed to give a

better frequency localization of the subcarriers. The prototype filter used in this paper is based on the frequency sampling technique [7]. This technique gives the advantage of using a closed-form representation that includes only a few adjustable design parameters.

The most significant parameter is the duration of the impulse response of the prototype filter also called overlapping factor, K. The impulse response of the prototype filter is given by [7]:

$$h(t) = G_P(0) + 2\sum_{k=1}^{K-1}(-1)^k G_P(k)\ cos\left(\frac{2\pi k}{KN}(t+1)\right) \tag{1}$$

where $G_P(0..3) = \left[1,\ 0.97195983,\ \frac{1}{\sqrt{2}},\ 1 - G_P(1)^2\right]$ for an overlapping factor of $K = 4$ and N is the number of carriers. The larger the overlapping factor K, the more localized the signal will be in frequency. Adjacent carriers significantly overlap with this kind of filtering. In order to keep adjacent carriers orthogonal, real and pure imaginary values alternate on successive carrier frequencies and on successive transmitted symbols for a given carrier at the transmitter side. In order to maximize spectral efficiency of the Offset QAM (OQAM) modulation the symbol period T is halved. The well-adjusted frequency localization of the prototype filter guarantees that only adjacent carriers interfere with each other. This allows for a more flexible operation than OFDM for FDMA access, i.e.: non synchronous flexible frequency division multiple access.

In [4], the authors describe a high performance receiver architecture denoted FS-FBMC (Frequency Spreading FBMC). One advantage of this architecture is that frequency domain time synchronization may be performed independently of the position of the FFT [4]. This is realized by combining timing synchronization with channel equalization. The proposed receiver architecture is depicted in Fig. 1. A free running FFT of size KN is processed every blocks of $N/2$ samples

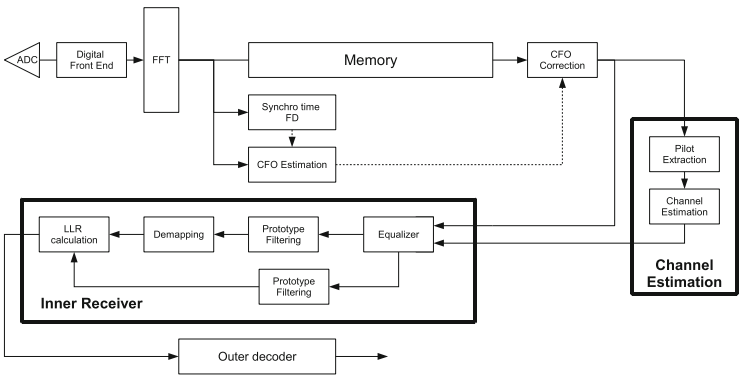

Fig. 1. Block diagram of the proposed receiver based on FS-FBMC principle. The time domain synchronization is performed in the frequency domain(box labelled "Synchro time FD").

generating KN points, i.e. if $\mathbf{r_m}$ is the m^{th} received vector, a KN-point FFT is computed for samples $k = (n + m \times N/2)$ with $n = 0, 1, \ldots, NK - 1$. These successive KN points are stored in a memory unit.

Assuming that the detection of a start of burst is then achieved on the frequency domain (i.e. at the output of the FFT) using a priori information from the preamble. The channel coefficients may be estimated on the pilot subcarriers of the preamble. Once the channel coefficients are estimated on all the active subcarriers, a one-tap per subcarrier equalizer is applied before filtering by the FBMC prototype filter. Demapping and Log-Likelihood Ratio (LLR) computation complete the inner receiver architecture. A soft-input Forward Error Correction (FEC) decoder finally recovers the original message.

The asynchronous frequency domain processing of the receiver combined with the high stop-band attenuation of the FBMC prototype filter provides a flexible receiver architecture that allows for multiuser asynchronous reception. FFT and Memory Unit are common modules, while the remaining of the receiver should be duplicated as many times as the number of parallel asynchronous users the system may tolerate. The originality of this paper lies in the fact that the time domain synchronization procedure is performed in the frequency domain and well adapted to this flexible scenario.

2.2 Burst Format

In order to keep a flexible frequency and time block allocation, a preamble based burst approach is considered. Synchronization and channel estimation is performed using a training sequence known to the receiver. Its structure has been defined and is illustrated in Fig. 2. It is composed of a preamble of duration P-FBMC symbols (P is set to 4 in Fig. 2). The preamble has been designed to accurately detect the start of the burst and gives an estimate of the channel

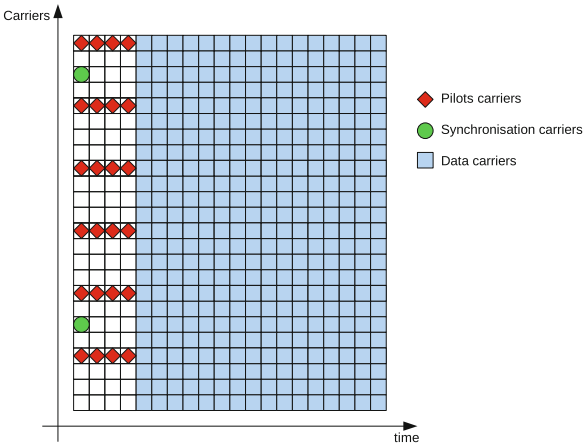

Fig. 2. Considered FBMC burst structure. (Color figure online)

frequency response while preserving the localization properties of the FBMC signal. It is mainly composed of pilot carriers spaced every D active carriers for the whole duration of the preamble (D is set to 4 in Fig. 2). The pilot carriers are designed so that the signal transmitted on each pilot carrier is constant for the duration of the preamble. Synchronization carriers are added on the first multicarrier symbol. These are designed to accurately estimate the start of burst as we will see after. By implementing at the receiver all the baseband signal processing functions in the frequency domain, the proposed scheme may be extended without loss of generalization to the aforementioned multiuser asynchronous environment.

In the following section, we will propose and evaluate signal processing algorithm for the detection of burst.

3 Time Synchronization

Time synchronization is the process by which the start of the burst is identified. In the proposed architecture, all the receiver signal processing operations are realized in the frequency domain. Consequently, the synchronization procedure should inform the other components of the receiver which block of samples, at the output of the FFT, corresponds to the beginning of the burst. Based on the structure of the preamble, a two-steps algorithm is realized. A coarse synchronization is performed followed by a fine synchronization procedure designed to accurately detect the start of the burst.

3.1 Coarse Time Synchronization

In this section, the metric for coarse frame detection in the frequency domain is introduced. A measure of the energy on the filtered carriers at specific carrier location is proposed. The decision metric is expressed as follows:

$$D_F(m) = \sum_{k \in \Omega_s} |y(k,m)|^2 \tag{2}$$

where Ω_s is the subset of carriers used for coarse synchronization and $y(k,m)$ is the received sample after prototype filtering at carrier index k and symbol m. The proposed algorithm is based on a classical hypothesis testing. We introduce the following two hypotheses:

- H_0 : only noise is received
- H_1 : signal plus noise is received

The decision whether a burst has been detected or not is realized on the rule:

$$D_F(m) > T \tag{3}$$

where T defines a threshold value. When this rule is true, the index m gives the reference time for the beginning of the burst. Two measures are usually studied

for the characterization of such an algorithm: the probability of false alarm P_{fa} and the probability of detection P_d. The probability of false alarm informs about the probability of a burst detection when only noise is received. The probability of detection gives the probability that a burst is detected when hypothesis H_1 occurs. The probability of false alarm is evaluated by analyzing the probability density function of the decision metric when H_0 occurs.

The analytic derivation of the false alarm probability as a function of the noise variance σ_n^2 and the cardinal of Ω_S, M, is well known and is given by [8]:

$$P_{fa}(T, M, \sigma_n^2) = \frac{\Gamma\left(M, \frac{T}{\sigma_n^2}\right)}{\Gamma(M)} \tag{4}$$

where T is the threshold and $\Gamma(x, y)$ is the upper incomplete gamma function:

$$\Gamma(x, y) = \int_y^{+\infty} t^{x-1} e^{-t} dt \tag{5}$$

This expression assumes independent noise following a normal distribution. A closed form expression for the probability of detection can be derived as [8]:

$$P_d(T, M, \sigma_s^2, \sigma_n^2) = Q_M\left(\sqrt{\frac{\sigma_s^2}{\sigma_n^2 M}}, \sqrt{\frac{T}{\sigma_n^2}}\right) \tag{6}$$

where σ_s^2 is the power of the useful signal. $Q(x, y)$ is the generalized Marcum-Q function.

We have evaluated the receiver operating characteristics (ROC) for the proposed detector when $M = 32$ and for various Carrier to Noise (C/N) ratio ($= \sigma_s^2/\sigma_n^2$). The size of the FFT is set to 256, and the synchronization preamble is built with 32 actives carriers. Simulations have been done assuming an AWGN (Additive white Gaussian Noise) channel. The C/N varies with a step of 1 dB starting from -5 dB. Due to the proposed receiver architecture and the synchronization process that is realized in the frequency domain, the FFT window is not synchronized with the emitted signal. Simulations have been done for a FFT position mismatch of $N/4$ samples. This is the worst case scenario as the signal energy leakage between consecutive FFT block is at its peak [4]. The coarse detector performance is given in Fig. 3. The probability of false alarm and the probability of misdetection are less than 10^{-2} for a C/N of 1 dB.

The main issue in classical detection problem resides in the determination of the decision threshold. The bottom graph in Fig. 3 illustrates the variation of the false alarm probability (resp. the misdetection probability) for various decision threshold values and for various C/N. For any given C/N a specific threshold that leads to the targeted false alarm probability can be derived (similarly for the misdetection probability).

In practice, it is not straightforward to compute the decision threshold as no information about hypothesis H_0 or H_1 is available. In order to propose a simpler practical realization, we modified the decision metric. We suggest computing

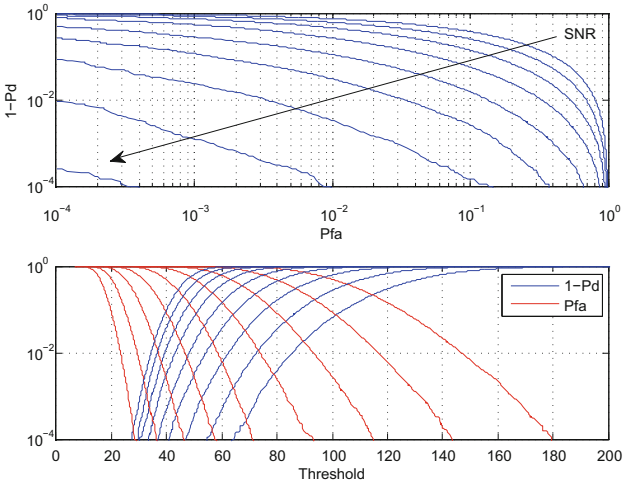

Fig. 3. Top: ROC curves for the proposed energy detector when $M = 32$ and for various SNR (resp C/N). The C/N varies with a step of 1 dB and starts at -5 dB. Bottom: variation of the false alarm probability and the misdetection probability in function of the threshold. (Color figure online)

on the same FFT block two physical observations in parallel. Energy level is computed at some carrier locations while an estimation of the noise is performed on other (null) carrier locations. Based on these two observations, we propose to build a metric by computing a likelihood ratio. We divide the power estimation at the carrier location by the power estimation at the null carrier positions. When H_0 occurs, the metric should tend to 1, and when H_1, the metric should be much greater than 1. The proposed metric can be defined as:

$$D_R(m) = \frac{|\Omega_n|}{|\Omega_s|} \frac{\sum_{k\in\Omega_s} |y(k,m)|^2}{\sum_{k\in\Omega_n} |y(k,m)|^2} \tag{7}$$

where Ω_n is the set of null carriers and $|\Omega_n|$ (resp. $|\Omega_s|$) is the number of element of the set Ω_n (resp. Ω_s) with $\Omega_s = M$. The analytic computation of a threshold is not straightforward to determine in this case because the metric is a division of chi-squared distribution. Consequently, simulations have been done to estimate the performances of the proposed receiver.

Here again, results have been simulated for the worst case scenario, i.e. a FFT misalignment of $N/4$ samples. Active carriers of the preamble are equally spaced every 4 carriers. The estimation of the noise is realized at the center of two successive synchronization carriers. We depict in Fig. 4 (a) the ROC curves when $M = 32$ and for various C/N.

Compared to the classical energy detection algorithm, the proposed scheme exhibits worse performance. This can be explained by the nature of the statistical test. The results show that for a C/N of 4 dB, the probability of false alarm and

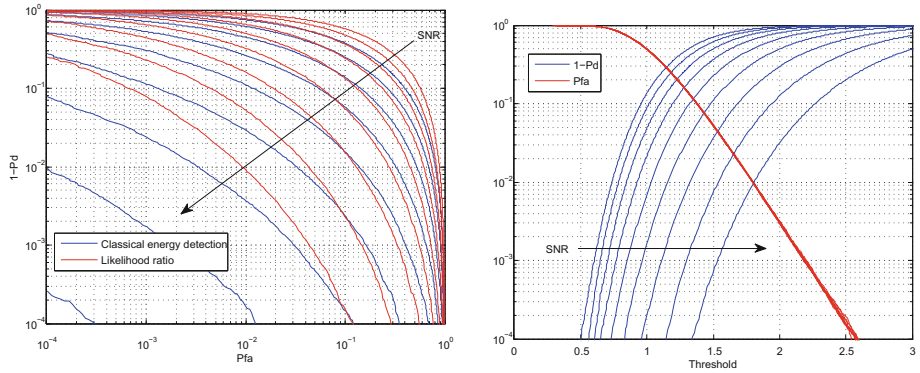

Fig. 4. (a) ROC curves for the proposed normalized energy detector using when $M = 32$ and for various C/N. The C/N varies with a step of 1 dB ans starts at -4 dB. (b) Variation of the false alarm probability and the misdetection probability for the proposed normalized energy detector using when $M = 32$ and for various C/N. The C/N varies with a step of 1 dB starting at -4 dB. (Color figure online)

the probability of misdetection is of around 10^{-2}. The advantage of this metric is depicted in Fig. 4 (b). The variation of the probability of false alarm and the probability of misdetection for various C/N as a function of a threshold is given. Here again a FFT with a misalignment of $N/4$ samples (worst case) is assumed.

We remark that thanks to the normalization, the decision threshold hardly depends on the SNR level (the variation is very small). For any C/N, a threshold equal to 2, leads to a false alarm probability smaller than 3.10^{-3}. The corresponding misdetection probability is lower than 10^{-2} for a C/N greater than 3 dB. Even if this metric suffers from a performance loss compared to the classical energy detection, the simplicity of the threshold determination makes this algorithm particularly interesting for practical realization of the coarse detection.

The evaluation of the performance has been done assuming an AWGN channel. In practice, fading channel affects the carrier. The knowledge of the fading positions are not available at the synchronization step: It is possible that at a given carrier position, only noise is present. Consequently when the number of active carriers is small performance of the proposed detectors is not sufficient.

The first improvement for the proposed algorithm consists of allocating more synchronization carriers. We illustrate in Fig. 5 the probability of misdetection when the false alarm probability is equal to 10^{-2} for various C/N values and various number of synchronization carriers. When we increase M, the number of synchronization carrier involved into the decision metric, performance is better. It should be mentioned that, in such a case, the threshold depends on M.

As dynamic spectrum usage is envisaged and possible multifrequency fragment, M can vary. Therefore it is interesting to establish a relationship between M and the synchronization threshold. We depict in Fig. 6 the variations of the

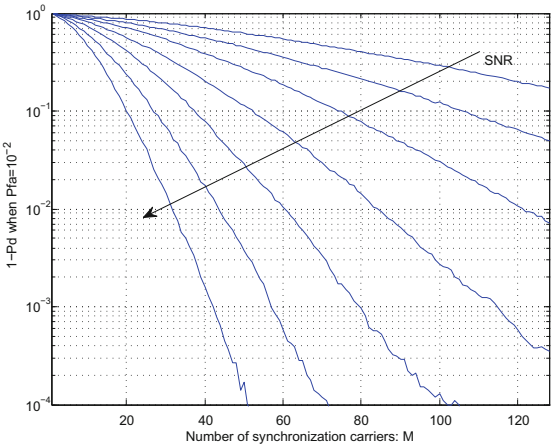

Fig. 5. Probability of misdetection when the false alarm probability is equal to 10^{-2} for various C/N values and various number of synchronization carriers. The C/N varies with a step of 1 dB starting at -4 dB.

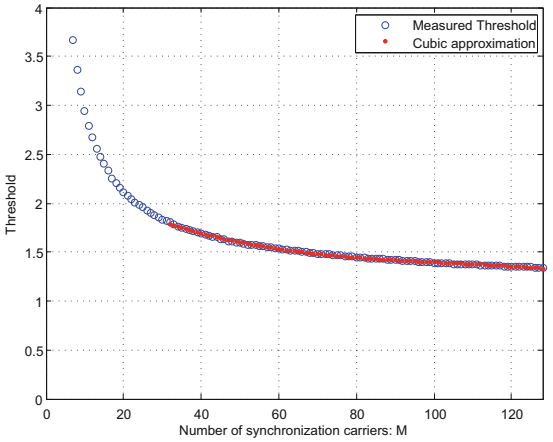

Fig. 6. Threshold values for a false alarm probability of 10^{-2} as a function of the number of synchronization carriers. (Color figure online)

threshold when the false alarm probability is set to 10^{-2} for different values of M. The threshold is a decreasing function of the number of synchronization carriers. It is useful for a flexible receiver to dynamically determine the threshold value according to the considered bandwidth for transmission. Under the assumption that the number of carriers dedicated to synchronization is in the range [32 128], we approximated the threshold value by a cubic function as follows:

$$T = -0.00000068M^3 + 0.000218M^2 - 0.024M + 2.358 \tag{8}$$

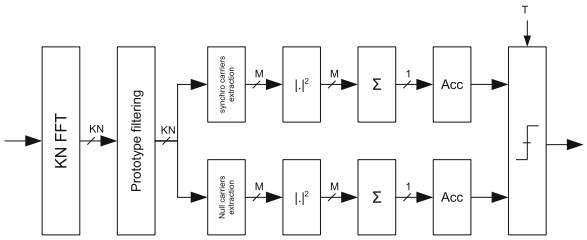

Fig. 7. Block diagram of the proposed coarse synchronization module.

This approximation allows for a simple and flexible computation of the threshold depending on the spectrum configuration.

The previous results have demonstrated that when the number of synchronization carriers is relatively small, performance is not really acceptable, especially if a margin on the C/N should be added to allow for performance over fading channels. If only a small fragment of spectrum is available for the transmission it is not possible to combine an important number of synchronization carriers (we have to keep in mind that null carriers without interference are required for noise estimation). The algorithm can be enhanced by exploiting the structure of the preamble and more precisely the repetition of the pilot carrier over time. The accumulation of different observations leads to better performance; this is effectively equivalent to increasing parameter M by time diversity.

The block diagram of the proposed synchronization module is depicted in Fig. 7. After the filtering in the frequency domain by the prototype filter, the power of each FFT block at synchronization (resp. null) carrier position is estimated and accumulated over successive blocks (Acc module). The two metrics are then compared using the decision threshold T to identify a coarse estimation of the start of the burst.

During the coarse detection, all the active carriers could be used for the energy estimation. More precisely, if we refer to the burst structure depicted in Fig. 2, the combination of the pilot and synchronization carriers may be used for the initial synchronization process. The coarse synchronization procedure is followed by a fine synchronization step designed to precisely identify the start of the burst.

3.2 Fine Time Synchronization

Fine time synchronization gives a refined position of the start of the burst. This step is essential for the signal processing operations that follow in the receiver chain such as channel estimation or equalization.

The proposed algorithm for fine time synchronization is based on the same principle as the one for the coarse time synchronization. The principle is to detect a power signature located at the beginning of the burst. While coarse

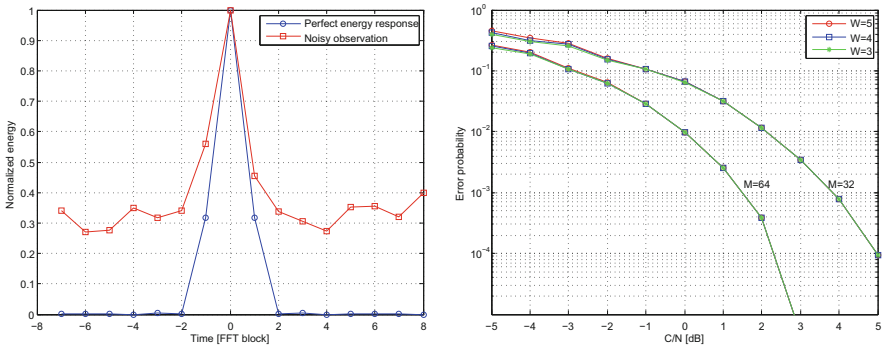

(a) (b)

Fig. 8. (a) Example of an energy signature for fine time synchronization. (b) Error probability of the proposed detector for various C/N. (Color figure online)

synchronization relies on the pilot carriers, only the synchronization carriers are used for fine synchronization (Fig. 2). Coarse synchronization is indeed optimized for misdetection and false alarm, while fine synchronization evaluates the most probable for the start of burst event instant. An example of the energy signature of a fine preamble sequence build on equi-distributed positions of the synchronization carriers is given in Fig. 8 (a).

Once coarse synchronization is acquired, we propose to lock the synchronization on the position corresponding to a maximum of energy. Therefore, we propose to evaluate the signal energy at the synchronization carrier location (see Fig. 2) using the following rule:

$$z(m) = \sum_{k \in \Omega_{Sync}} |y(k,m)|^2 \tag{9}$$

$$\hat{m} = \max_{m \in W} z(m) \tag{10}$$

where W is the set of position to test and Ω_{Sync} is the set of synchronization carriers indexes. It should be mentioned that the fine time synchronization can be directly applied. However, the use of a robust coarse synchronization based on a higher number of observations (the number of pilot carrier is higher than the number of synchronization carrier) gives better performance.

The performance of the proposed detector has been evaluated by simulation over an AWGN channel. We depict in Fig. 8 (b) the error probability for various C/N. An error is assumed when the position at the output of the detector is not correct. These results show that the size of the window (W) has a limited impact on the performances especially at high C/N region. When the number of carriers used for the energy detection increases, performance also increases. Maximizing the number of synchronization carriers while maintaining orthogonality between the pattern is crucial to guarantee good performance.

4 Conclusion

In this work, a frequency agile time domain synchronization algorithm adapted to dynamic fragmented spectrum scenarios in a multiuser context has been addressed. The detection of the start of multicarrier frame algorithm is based on detecting the power signature of a preamble sequence. The procedure is divided into two steps, a coarse followed by a fine acquisition step. Performance and practical realization have been discussed and evaluated. An efficient architecture with an associated threshold determination method adapted to the dynamic scenario has been proposed. The method not only performs well for low C/N but is also very adapted to dynamic access per user as its decision threshold can be efficiently predicted according to the amount of occupied spectrum.

Acknowledgment. This work has been carried out in the frame of the PROFIL project, which is funded by the French National Research Agency (ANR) under the contract number ANR-13-INFR-0007-02.

References

1. Wunder, G., et al.: 5GNOW: Challenging the LTE design paradigms of orthogonality and synchronicity. In: 2013 IEEE 77th Vehicular Technology Conference (VTC Spring) (2013)
2. Noguet, D., Gautier, M., Berg, V.: Advances in opportunistic radio technologies for TVWS. EURASIP J. Wirel. Commun. Netw. **2011**(1), 170 (2011). http://jwcn.eurasipjournals.com/content/2011/1/170
3. Medjahdi, Y., Terre, M., Le Ruyet, D., Roviras, D.: On spectral efficiency of asynchronous OFDM/FBMC based cellular networks. In: IEEE 22nd International Symposium on Personal Indoor and Mobile Radio Communications (PIMRC), pp. 1381–1385, September 2011
4. Doré, J., Berg, V., Cassiau, N., Kténas, D.: FBMC receiver for multi-user asynchronous transmission on fragmented spectrum. EURASIP J. **2014**, 1–41 (2014). Special Issue on Advances in Flexible Multicarrier Waveform for Future Wireless Communications
5. Speth, M., Fechtel, S., Fock, G., Meyr, H.: Optimum receiver design for wireless broad-band systems using OFDM. I. IEEE Trans. Commun. **47**(11), 1668–1677 (1999)
6. Schmidl, T., Cox, D.: Robust frequency and timing synchronization for OFDM. IEEE Trans. Commun. **45**(12), 1613–1621 (1997)
7. Bellanger, M., et al.: FBMC physical layer: a primer (2010). http://www.ict-phydyas.org
8. Salehi, M., Proakis, J.: Digital Communications. McGraw-Hill Education, New York (2007)